PHYSICAL REVIEW B **76**, 060403(R) (2007)

Microscopic aspect of interface magnetic anisotropy induced by a Pd adlayer on Ni/Cu(001) films

J.-S. Lee,[1] J.-Y. Kim,[2] J. H. Shim,[1] B. I. Min,[1] K.-B. Lee,[1,2] and J.-H. Park[1,2,*]
[1]*eSSC & Department of Physics, Pohang University of Science and Technology, Pohang 790-784, Korea*
[2]*Pohang Accelerator Laboratory, Pohang University of Science and Technology, Pohang 790-784, Korea*
(Received 3 June 2007; published 8 August 2007)

We performed comprehensive studies on the magnetic influence of a thin (5 Å) Pd adlayer on epitaxial Ni/Cu films using x-ray magnetic circular dichroism (XMCD) at the Ni $L_{2,3}$ and Pd $M_{2,3}$ edges. The magnetic anisotropy was found to be greatly affected by the adlayer. The XMCD shows that the orbital magnetic moment m_o of Ni is enhanced and a considerable magnetic moment is induced at Pd, resulting in an interface magnetic anisotropy, which well explains the anisotropy changes. We also found that a certain amount of charges are transferred from Pd 4*d* to Ni 3*d* at the interface. The transferred charges mainly reduce the weight of the Ni $3d^8$ state and increase m_o.

DOI: 10.1103/PhysRevB.76.060403 PACS number(s): 75.70.−i, 75.30.Gw, 78.70.Dm

Magnetic anisotropy is a subject of great interest in magnetic thin films, and extensive efforts have been made to obtain perpendicular magnetic anisotropy (PMA) as needed for high-density magnetic storage devices and magneto-optical recording media.[1–4] The magnetic anisotropy of a film, which determines the preferred magnetization direction, results from competition between magnetostatic, surface magnetic, and magnetocrystalline anisotropy. The magnetostatic energy corresponds to a magnetic dipole-dipole interaction and favors in-plane anisotropy.[5] The surface magnetic[6] and magnetocrystalline energies,[7] which result from spin-orbit coupling of surviving orbital momenta at the surface and bulk, respectively, yield either in-plane or perpendicular anisotropy depending on the orbital momentum direction.[8]

Meanwhile the orbital momentum has been found to be modified by lattice strain as well as by a Pd or Pt nonmagnetic adlayer.[9] The strain, which is induced by lattice mismatch with the substrate, contributes an additional orbital momentum by compressing the orbital states, and affects the magnetic anisotropy, the so-called magnetoelastic anisotropy.[10] However, the adlayer effect on the magnetic anisotropy, the so-called interface magnetic anisotropy (IMA),[11] is not well understood and its fundamental mechanism has never been fully investigated. IMA has been observed in various systems such as Pd/Fe, Pd/Co, Pt/Co, Pt/Ni, etc., with a great enhancement of the orbital magnetic moment m_o.[12] The enhancement was considered to be due to symmetry breaking at the interface[13] but the estimated value is at least an order of magnitude smaller than the observed one.[14,15] Further, the enhanced m_o did not fully account for the adlayer effect, and the IMA was simply attributed to a hybridization effect at the interface.[16]

In this paper, we present results of comprehensive studies on the interface magnetic anisotropy induced by a Pd adlayer on Ni/Cu(001) films using x-ray magnetic circular dichroism (XMCD) and x-ray absorption spectroscopy (XAS) at the Ni $L_{2,3}$ edges, and clarify its microscopic mechanism. The adlayer turns out to affect the magnetic hysteresis (M vs H) curve, and XMCD showed a great enhancement of m_o at Ni. In the XAS spectrum, the intensity of the 6 eV satellite, which originates from a $3d^8$ configuration in the ground state,[17] becomes reduced with the adlayer, indicating Pd 4*d* to Ni 3*d* charge transfer. Further, in studies on a Pd-Ni multilayer and an alloy, in which the ratio of the Pd-Ni interface increases, we found that m_o increases dramatically, and the satellite intensity mostly disappears. Meanwhile, we observed a considerable MCD signal at the Pd $M_{2,3}$ edge, which represents a magnetic moment of Pd 4*d* induced by strong Pd 4*d*–Ni 3*d* bonding at the interface. We finally found that IMA is well explained in terms of the induced Pd magnetic moment and the enhanced Ni orbital moment, which affect PMA in opposite ways.

A Cu(001) substrate was cleaned through cycles of Ne^+ sputtering and annealing at 900 K, and 15-, 30-, and 60-Å-thick Ni films were grown epitaxially in a wedge shape on the substrate at 300 K. During the growth, the pressure was maintained at $\sim 4\times 10^{-10}$ Torr. The growth rate was about 1 Å/min., and the epitaxy of the film was confirmed by the low-energy electron diffraction pattern. Then a 5-Å-thick Pd layer was deposited on the Ni wedge. The strain and thicknesses of the films were checked *ex situ* by using x-ray diffraction and reflectivity, respectively. XAS and XMCD were measured with 98% linearly and 95% circularly polarized incident light, respectively, at the elliptically polarized undulator beamline 2A in the Pohang Light Source (PLS). The energy resolution was set to be 0.3 eV. The spectra were collected in total electron yield mode at 300 K.

Figure 1 shows magnetic hysteresis (M vs H) curves of the 15-, 30-, and 60-Å-thick Ni films on Cu(001) along the out-of-plane direction before and after Pd deposition. The M vs H curves were obtained by monitoring the XMCD intensity at the Ni L_3 white line. Before the deposition, all three films show PMA, and the coercive field increases with increase of the film thickness. As discussed previously,[18] the magnetic anisotropy is determined by the competition between surface magnetic anisotropy, magnetostatic anisotropy, and magnetoelastic anisotropy induced by the tensile strain (2.5% lattice mismatch between Ni and Cu). For a very small Ni thickness below ~10 Å, the film shows in-plane anisotropy due to large negative surface anisotropy. As the film thickness increases, the anisotropy is dominated by a large magnetoelastic anisotropy and becomes PMA in a range of

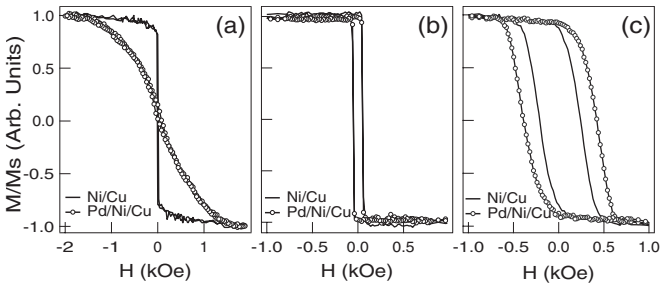

FIG. 1. Out-of-plane M vs H curves: (a) Ni(15 Å)/Cu, (b) Ni(30 Å)/Cu, and (c) Ni(60 Å)/Cu before and after Pd-layer deposition.

10–100 Å. Hence PMA is barely preserved in the Ni(15 Å)/Cu film, and the coercive field becomes nearly minimal. For large film thickness, the PMA becomes stronger and the coercive field is enhanced as seen in the figure. For larger thickness above 100 Å, the magnetostatic anisotropy changes back to in-plane anisotropy.

After Pd deposition, the M vs H curves change differently for different thicknesses. In the 15 Å film, the magnetic easy axis switches from the out-of-plane to the in-plane direction, while almost no change occurs in the 30 Å film. In the 60 Å film, the coercive field greatly increases and PMA is reinforced. These changes indicate that the adlayer makes a great influence on the magnetic anisotropy although Pd itself is nonmagnetic.

To explore microscopically the magnetic influence of the adlayer, we performed Ni $L_{2,3}$ edge XMCD measurements, which provide quantitative information on element-specific spin and orbital magnetic moments.[20,21] A 0.5 T pulse magnet switched the remanent magnetization along the normally incident direction at each data point. The absorption spectra for different magnetization directions parallel and antiparallel to the photon helicity vector (ρ_+ and ρ_-), and the dichroism ($\Delta\rho$) and its integration for Ni(60 Å)/Cu are shown in Fig. 2(a). The spectra (ρ_+ and ρ_-), which result from Ni $2p \rightarrow 3d$ dipole transitions, are divided roughly into L_3 ($2p_{3/2}$) and L_2 ($2p_{1/2}$) regions. The integration of $\Delta\rho$ over the entire $L_{2,3}$ region is proportional to the orbital magnetic moment. By using the sum rule,[20,21] the spin (m_s) and orbital (m_o) moments, which are parallel to each other, are estimated as $0.65\pm0.03\mu_B$/Ni and $0.068\pm0.004\mu_B$/Ni, respectively, giving a ratio of $m_o/m_s=0.105$, in good agreement with those of a bulklike thick Ni film.[19]

Figure 2(b) shows the XAS spectra ($\rho_+ + \rho_-$) and their integration after removing absorption edge jumps[21] of Ni/Cu films before and after Pd deposition. The integration, which corresponds to the Ni $3d$ hole number, shows about 14±3 % reduction for the 15 Å Ni film after the deposition.[22] The reduction slightly decreases with increase of the film thickness, and is 11±3 % for the 60 Å Ni film, indicating that the reduction mostly occurs within a few monolayers at the interface. The hole number in bulk Ni was estimated to be 0.9–1.0 both theoretically and experimentally,[17] and 14% reduction corresponds to an increase of 0.12–0.14 electrons per Ni, which are expected to be transferred from Pd.

Figure 2(c) shows the dichroism ($\Delta\rho=\rho_+-\rho_-$) of Ni/Cu and Pd/Ni/Cu films, which were obtained with the remanent magnetization normal to the plane. For Pd/Ni(15 Å)/Cu, in which the easy axis is in the plane, in-plane measurements were also performed. As can be seen in the figure, the dichroisms of all three Ni/Cu films were modified by the Pd adlayer. Interestingly, the change is even considerable for the 30 Å film, whose M vs H curve barely changes with deposition of the adlayer. The relatively large decrease in the L_2 region indicates a certain enhancement of m_o. Before the Pd deposition, the spin moment was estimated to be nearly the same for all three Ni/Cu films, $m_s \simeq 0.65\mu_B$/Ni, while $m_o=0.083\pm0.004\mu_B$/Ni and $0.068\pm0.004\mu_B$/Ni for Ni(15 Å)/Cu and Ni(30 Å)/Cu, 22% and 0% larger than that of Ni(60 Å)/Cu, respectively. This increase is known to be due to the magnetoelastic anisotropy at the Ni/Cu interface as mentioned above.[18] The interface effect is greatly reduced with increase of the Ni thickness, and becomes negligible even in Ni(30 Å)/Cu. This is because the penetration depth of the measurement is about 30 Å and the estimated moments reflect only this length scale from the top surface.

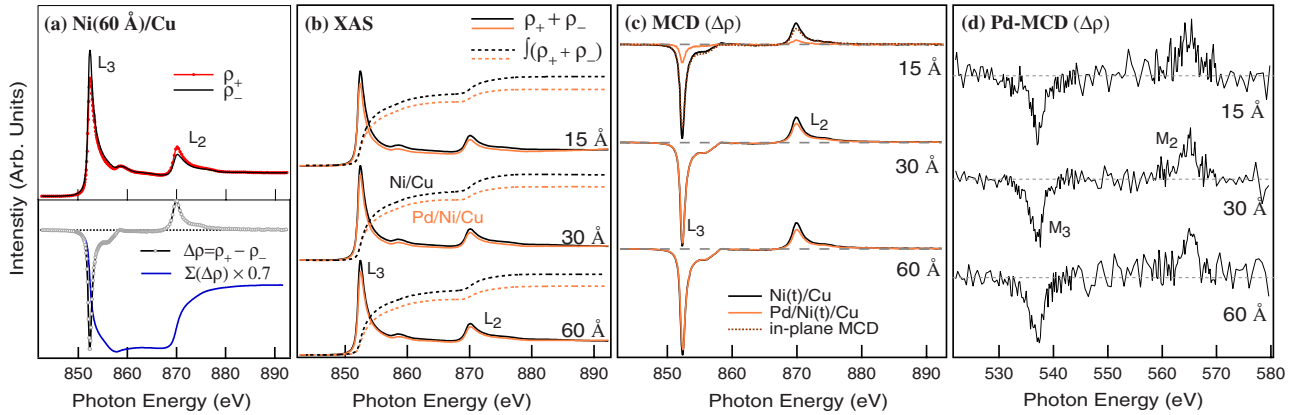

FIG. 2. (Color online) (a) Ni $L_{2,3}$ edge XMCD spectra (ρ_+ and ρ_-), MCD ($\Delta\rho$), and its integration, $\Sigma(\Delta\rho)$, of Ni(60 Å)/Cu. (b) total XAS, $\rho_+ + \rho_-$, and its integration, $\int(\rho_+ + \rho_-)$, of Ni/Cu and Pd/Ni/Cu with 15, 30, and 60 Å Ni thicknesses. (c) Out-of-plane MCD spectra before and after the Pd-layer deposition. The in-plane MCD is additionally given for Pd/Ni(15 Å)/Cu. (d) MCD signal of Pd/Ni/Cu at Pd $M_{2,3}$ edges. It was obtained in a persistent magnetization mode in Pd/Ni(15 Å)/Cu.

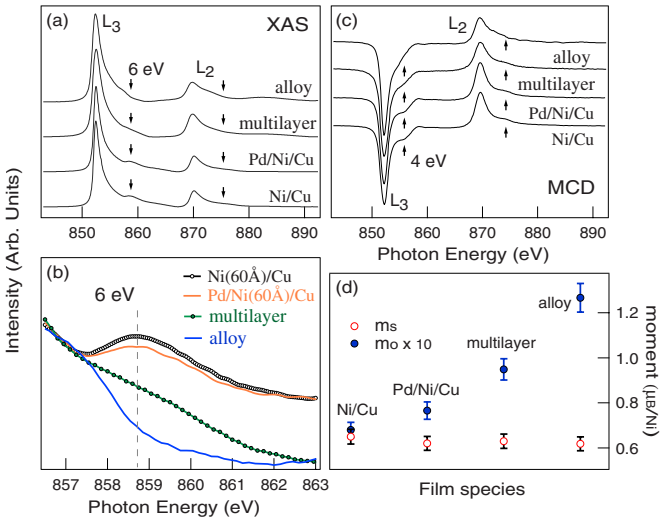

FIG. 3. (Color online) (a) Ni $L_{2,3}$ XAS spectra, (b) the 6 eV satellite feature in the L_3 region, (c) the Ni $L_{2,3}$ MCD spectra, and (d) the estimated magnetic moments (m_s and m_o) of Ni(60 Å)/Cu, Pd/Ni(60 Å)/Cu, a Pd/Ni multilayer, and a PdNi alloy. The 6 eV and 4 eV satellites are indicated by arrows in (a) and (c), respectively.

After Pd deposition, m_s decreases by about 4% ($0.03\mu_B$/Ni) while m_o increases by about 10% ($0.008-0.007)\mu_B$/Ni for all three films, resulting in an enhancement of m_o/m_s. Considering that the amount of the transferred charges is as large as 0.10–0.14 per Ni, such a small reduction in m_s is rather surprising.

To examine the electronic changes accompanying the Pd adlayer, we performed linear muffin-tin orbital band calculations in the local spin density approximation on bulk Ni and a Pd(5 monolayers)/Ni(5 monolayers) bilayer.[23] The number of Ni d holes in the bilayer was estimated as 0.82/Ni, which is 11% smaller than the hole number (0.92/Ni) in the bulk Ni. m_s decreases by 2% and m_o increases by 7%, consistently with the XMCD results. Ni 3d states strongly bond with Pd 4d states, and the bonding makes the 3d band broader and shifts it down energetically. The energy shift reduces the number of Ni 3d holes considerably. But, due to the band broadening, the reductions in the up and down spin holes become similar and the change in m_s is rather tiny. These results suggest that the Pd adlayer induces not only Ni to Pd charge transfer but also strong Ni 3d–Pd 4d bonding, which distorts Ni 3d orbitals and increases the orbital angular momentum.

The Pd 4d states strongly hybridize with the Ni 3d states and become spin polarized. Figure 2(d) shows Pd $M_{2,3}$ MCD of Pd/Ni(15 Å)/Cu, Pd/Ni(30 Å)/Cu, and Pd/Ni(60 Å)/Cu. The MCD signal shows that the Pd magnetic moment is parallel to that of Ni since the hybridization keeps the spin configuration. The signal is rather noisy due to the small absorption cross section, and we could not extract reliable Pd magnetic moments because of the low signal-to-noise ratio. According to the band calculation, the magnetic moment of Pd is estimated to be as large as $0.20\mu_B$/Pd ($m_s=0.18\mu_B$ and $m_o=0.02\mu_B$), consistent with

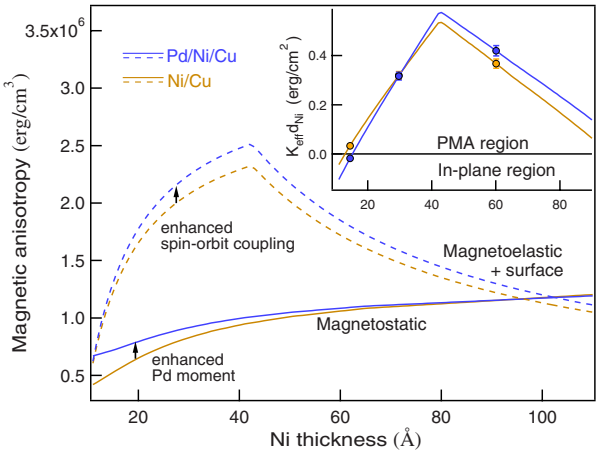

FIG. 4. (Color online) Magnetic anisotropies $K_{MS}=2\pi M_s^2$ and $K_{ME}+K_S/d_{Ni}$ vs d_{Ni} of Ni/Cu and Pd/Ni/Cu films. Ni/Cu data are taken from Ref. 18. Up arrows indicate shifts in magnetic anisotropy due to Pd adlayer. Inset shows effective magnetic anisotropy $K_{eff}d_{Ni}$.

the Pd moment of Ni/Pd multilayers reported previously.[24] Considering the induced Pd moment, the Pd adlayer enhances both spin and orbital moments of the whole film.

To scrutinize the Pd-Ni interface effect on electronic states, we prepared samples with various Pd-Ni environments, such as Ni(60 Å)/Cu, Pd/Ni(60 Å)/Cu, a $[Pd(5\text{ Å})/Ni(5\text{ Å})]_{10}$ multilayer, and a $Pd_{0.5}Ni_{0.5}$ alloy, and performed Ni $L_{2,3}$ edge XAS and XMCD measurements. The Ni-Pd interface (Ni-Pd bond) ratio is supposed to monotonically increase in the sequence of Ni, Pd/Ni, Pd/Ni multilayer, and Pd-Ni alloy. As shown in Figs. 3(a) and 3(c), the XAS and MCD spectra exhibit the so-called 6 eV (XAS) and 4 eV (MCD) satellites additional to the $L_{2,3}$ main features. Those are known to originate, respectively, from singlet and triplet $2p^63d^8 \rightarrow 2\underline{p}^5 3d^9$ transitions, besides the main $2p^63d^9 \rightarrow 2\underline{p}^5 3d^{10}$.[17] The ground state of bulk Ni can be presented as a linear combination of $3d^8$, $3d^9$, and $3d^{10}$ configuration states, and their relative weights were estimated to be 15–20 %, 50–60 %, and 25–30 %, respectively.[17] Remarkably, the intensity of the XAS 6 eV satellite decreases with increase of the interface ratio, as shown in Fig. 3(b). The intensity is considerable in Ni(60 Å)/Cu as in the bulk,[19] while it becomes barely observable in the Pd/Ni multilayer and alloy. A similar decreasing behavior is also observable in the intensity of the MCD 4 eV satellite. The Pd 4d to Ni 3d charge transfer at the interface causes a prominent decrease of the weight of the $3d^8$ state in the ground state.

Further, as the interface ratio increases, m_o of Ni increases dramatically while m_s barely changes, as shown in Fig. 3(d). Configuration interaction analysis for XAS spectra of Ni metal and multilayers show that the $3d^8$ weight mostly switches into $3d^{10}$, while the $3d^9$ weight barely changes. This is because the amount of $3d^8 \rightarrow 3d^9$ transfer is about the same as that of $3d^9 \rightarrow 3d^{10}$. The weight of the singlet $3d^8$, which does not contribute to the MCD signal, overwhelms that of the triplet $3d^8$ in the ground state,[17] and the charge transfer results in a tiny change of m_s. These findings are consistent with the band calculation results that the Ni 3d

orbital becomes distorted by the Ni $3d-$Pd $4d$ bonding and the orbital angular momentum of the $3d^9$ is greatly enhanced.

Our results show that the Pd adlayer enhances both the spin and orbital moments of the whole film. Such enhancements contribute an additional magnetic anisotropy, the interface magnetic anisotropy. Now let us reconsider the Pd adlayer effects—the changes in M vs H curves shown in Fig. 1. For quantitative analyses, magnetic anisotropy coefficients were estimated from the experimental results.[18] Figure 4 presents estimations for the magnetostatic anisotropy $K_{\mathrm{MS}}=2\pi M_s^2$ and the sum of the magnetoelastic (K_{ME}) and surface magnetic anisotropy (K_S/d_{Ni}) (Ref. 25) on Ni/Cu and Pd/Ni/Cu films. M_s denotes the total spin moment. The surface anisotropy energy per unit volume depends on the Ni thickness d_{Ni}. The coefficients for Ni/Cu films were taken from Ref. 18. Upon depositing the Pd adlayer, the enhanced m_o increases $K_{\mathrm{ME}}+K_S/d_{\mathrm{Ni}}$, which comes from the spin-orbit coupling energy, and reinforces PMA, while the enhanced M_s increases K_{MS} for a given d_{Ni}, by $2\pi M_{\mathrm{Pd}}^2 d_{\mathrm{Pd}}/(d_{\mathrm{Ni}}+d_{\mathrm{Pd}})$ and suppresses PMA. Here M_{Pd} and d_{Pd} denote the magnetic moment and thickness of the Pd layer, respectively.[26,27] As can be seen in Fig. 1, IMA barely affects the magnetic anisotropy in Pd(5 Å)/Ni(30 Å)/Cu, indicating that increase in $K_{\mathrm{ME}}+K_S/d_{\mathrm{Ni}}$, which is expected to be independent of d_{Ni}, nearly cancels that in K_{MS}. But increase in K_{MS} is more effective at smaller d_{Ni}, and thus in Pd(5 Å)/Ni(15 Å)/Cu, K_{MS} surpasses $K_{\mathrm{ME}}+K_S/d_{\mathrm{Ni}}$, i.e., IMA suppresses PMA, while the situation becomes opposite in Pd(5 Å)/Ni(60 Å)/Cu, i.e., IMA reinforces PMA. The resulting effective magnetic anisotropy ($K_{\mathrm{eff}}=-K_{\mathrm{MS}}+K_{\mathrm{ME}}+K_S/d_{\mathrm{Ni}}$) is compared for Ni/Cu and Pd/Ni/Cu in the inset of Fig. 4. The suppression of PMA switches the easy axis of Ni(15 Å)/Cu, in which PMA was barely preserved. The reinforcement of PMA in Ni(60 Å)/Cu increases the coercive field. Such influences of IMA well explain the observed changes in M vs H curves for different d_{Ni}.

In summary, we investigated the interface magnetic anisotropy induced by a Pd adlayer on Ni/Cu(001) films, and clarified its microscopic mechanism. The Ni orbital moment is enhanced and a considerable amount of magnetic moment is induced at Pd, resulting in modification of the magnetic anisotropy. These changes are accompanied by a large Pd $4d$ to Ni $3d$ charge transfer at the interface. The Ni $3d$ orbital becomes distorted by strong Ni $3d-$Pd $4d$ bonding, and the orbital angular momentum of $3d^9$ is greatly enhanced.

This work was supported by KOSEF through the eSSC at POSTECH, KRF Grant No. KRF-2006-312-C00523, POSTECH research fund, and BK21 Program. PAL is supported by POSTECH and MOST.

*Correspondence should be addressed to jhp@postech.ac.kr

[1] U. Gradmann, J. Magn. Magn. Mater. **54**, 733 (1986).
[2] D. S. Chuang, C. A. Ballentine, and R. C. O'Handley, Phys. Rev. B **49**, 15084 (1994).
[3] D. Weller, J. Stöhr, R. Nakajima, A. Carl, M. G. Samant, C. Chappert, R. Megy, P. Beauvillain, P. Veillet, and G. A. Held, Phys. Rev. Lett. **75**, 3752 (1995).
[4] H. A. Dürr, G. Y. Guo, G. van der Laan, J. Lee, G. Lauhoff, and J. A. C. Bland, Science **277**, 213 (1997).
[5] H. J. G. Draaisma and W. J. M. de Jonge, J. Appl. Phys. **64**, 3610 (1988).
[6] U. Gradmann, *Handbook of Magnetic Materials* (Elsevier, Amsterdam, 1993), Vol. 7, p. 27, and references therein.
[7] R. Wu and A. J. Freeman, J. Magn. Magn. Mater. **200**, 498 (1999).
[8] J. Stöhr and H. König, Phys. Rev. Lett. **75**, 3748 (1995).
[9] P. F. Carcia, A. D. Meinhaldt, and A. Suna, Appl. Phys. Lett. **47**, 178 (1985); B. Hillebrands and J. R. Dutcher, Phys. Rev. B **47**, 6126 (1993).
[10] R. Jungblut, M. T. Johnson, J. aan de Stegge, A. Reinders, and F. J. A. den Broeder, J. Appl. Phys. **75**, 6424 (1994); G. Lauhoff, C. A. F. Vaz, J. A. C. Bland, J. Lee, and T. Suzuki, Phys. Rev. B **61**, 6805 (2000).
[11] G. Bochi, C. A. Ballentine, H. E. Inglefield, C. V. Thompson, and R. C. O'Handley, Phys. Rev. B **53**, R1729 (1996); J.-S. Lee, K.-B. Lee, Y. J. Park, T. G. Kim, J. H. Song, K. H. Chae, J. Lee, C. N. Whang, K. Jeong, D.-H. Kim, and S.-C. Shin, *ibid.* **69**, 172405 (2004).
[12] Y. Wu, J. Stöhr, B. D. Hermsmeier, M. G. Samant, and D. Weller, Phys. Rev. Lett. **69**, 2307 (1992); S.-K. Kim and J. B. Kortright, *ibid.* **86**, 1347 (2001); X. LeCann, C. Boeglin, B. Carriere, and K. Hricovini, Phys. Rev. B **54**, 373 (1996).
[13] L. Néel, J. Phys. Radium **15**, 225 (1954).
[14] G. H. O. Daalderop, P. J. Kelly, and M. F. H. Schuurmans, Phys. Rev. B **41**, 11919 (1990).
[15] R. C. O'Handley, *Modern Magnetic Materials: Principles and Applications* (John Wiley & Sons, New York, 2000).
[16] D. S. Wang, R. Wu, and A. J. Freeman, Phys. Rev. B **47**, 14932 (1993).
[17] T. Jo and G. A. Sawatzky, Phys. Rev. B **43**, 8771 (1991); L. H. Tjeng, C. T. Chen, P. Rudolf, G. Meigs, G. van der Laan, and B. T. Thole, *ibid.* **48**, 13378 (1993); G. van der Lann and B. T. Thole, J. Phys.: Condens. Matter **4**, 4181 (1992).
[18] W. L. O'Brien, T. Droubay, and B. P. Tonner, Phys. Rev. B **54**, 9297 (1996).
[19] K. Amemiya, E. Sakai, D. Matsumura, H. Abe, T. Ohta, and T. Yokoyama, Phys. Rev. B **71**, 214420 (2005); C. T. Chen, F. Sette, Y. Ma, and S. Modesti, *ibid.* **42**, 7262 (1990).
[20] B. T. Thole, P. Carra, F. Sette, and G. van der Laan, Phys. Rev. Lett. **68**, 1943 (1992).
[21] C. T. Chen, Y. U. Idzerda, H.-J. Lin, N. V. Smith, G. Meigs, E. Chaban, G. H. Ho, E. Pellegrin, and F. Sette, Phys. Rev. Lett. **75**, 152 (1995).
[22] Distortion in the Ni L edge jump background due to the 5-Å-thick Pd layer turns out to be even less than the estimation error.
[23] The number of Ni d holes in a Ni (5 monolayers) film was estimated to be about the same as those in bulk Ni.
[24] J.-R. Jeong and S.-C. Shin, Appl. Phys. Lett. **75**, 3174 (1999).
[25] K_S is from the two-dimensionality and sometimes divided into the anisotropies for the Ni surface and Ni/Cu interface.
[26] D. Weller, Y. Wu, J. Stöhr, M. G. Samant, B. D. Hermsmeier, and C. Chappert, Phys. Rev. B **49**, 12888 (1994).
[27] L. Cheng, Z. Altounian, D. H. Ryan, J. O. Strom-Olsen, M. Sutton, and Z. Tun, Phys. Rev. B **69**, 144403 (2004).